

Accepted Manuscript

Design of Ru(II) sensitizers endowed by three anchoring units for adsorption mode and light harvesting optimization

Maria Grazia Lobello, Simona Fantacci, Norberto Manfredi, Carmine Coluccini, Alessandro Abbotto, Mohammed K. Nazeeruddin, Filippo De Angelis

PII: S0040-6090(13)01425-9
DOI: doi: [10.1016/j.tsf.2013.08.112](https://doi.org/10.1016/j.tsf.2013.08.112)
Reference: TSF 32540

To appear in: *Thin Solid Films*

Received date: 8 June 2013
Revised date: 23 August 2013
Accepted date: 30 August 2013



Please cite this article as: Maria Grazia Lobello, Simona Fantacci, Norberto Manfredi, Carmine Coluccini, Alessandro Abbotto, Mohammed K. Nazeeruddin, Filippo De Angelis, Design of Ru(II) sensitizers endowed by three anchoring units for adsorption mode and light harvesting optimization, *Thin Solid Films* (2013), doi: [10.1016/j.tsf.2013.08.112](https://doi.org/10.1016/j.tsf.2013.08.112)

This is a PDF file of an unedited manuscript that has been accepted for publication. As a service to our customers we are providing this early version of the manuscript. The manuscript will undergo copyediting, typesetting, and review of the resulting proof before it is published in its final form. Please note that during the production process errors may be discovered which could affect the content, and all legal disclaimers that apply to the journal pertain.

Design of Ru(II) sensitizers endowed by three anchoring units for adsorption mode and light harvesting optimization

Maria Grazia Lobello,^a Simona Fantacci,^a Norberto Manfredi,^b Carmine Coluccini,^b Alessandro Abbotto,^{b,} Mohammed K. Nazeeruddin,^{c,*} Filippo De Angelis,^{a,*}*

^aComputational Laboratory for Hybrid/Organic Photovoltaics (CLHYO), Istituto CNR di Scienze e Tecnologie Molecolari, Via elce di Sotto 8, I-06213, Perugia, Italy.

^bDepartment of Materials Science and Milano-Bicocca Solar Energy Research Center - MIB-Solar, University of Milano-Bicocca and INSTM, Via Cozzi 53, I-20125, Milano, Italy. E-mail:

^cLaboratory for Photonics and Interfaces, Station 6, Institute of Chemical Sciences and Engineering, School of basic Sciences, Swiss Federal Institute of Technology, CH - 1015 Lausanne, Switzerland.

Corresponding authors:

Filippo De Angelis: filippo@thch.unipg.it, phone: +390755855523

Alessandro Abbotto: alessandro.abbotto@unimib.it

Mohammed K. Nazeeruddin: mdkhaja.nazeeruddin@epfl.ch

Abstract:

We report the design, synthesis and computational investigation of a class of Ru(II)-dyes based on mixed bipyridine ligands for use in dye-sensitized solar cells. These dyes are designed to preserve the optimal anchoring mode of the prototypical N719 sensitizer by three carboxylic groups, yet allowing for tunable optimization of their electronic and optical properties by selective substitution at one of the 4-4' positions of a single bipyridine ligand with π -excessive heteroaromatic groups. We used Density Functional Theory/ Time Dependent Density Functional Theory calculations to analyze the electronic structure and optical properties of the dye and to investigate the dye adsorption mode on a TiO₂ nanoparticle model. Our results show that we are effectively able to introduce three carboxylic anchoring units into the dye and achieve at the same time an enhanced dye light harvesting, demonstrating the design concept. As a drawback of this type of dyes, the synthesis leads to a mixture of dye isomers, which are rather tedious to separate.

Keywords

Ru(II) dyes, Density functional calculations, UV/Vis spectroscopy, Dye adsorption on TiO₂.

1. Introduction

Dye-sensitized Solar Cells (DSCs) are promising alternatives to conventional photovoltaics for the direct conversion of solar energy into electricity at low cost and with high efficiency[1-6]. In DSCs, a dye sensitizer, adsorbed on the surface of a mesoporous nanostructured semiconductor film, usually made of titanium dioxide (TiO_2), absorbs the solar radiation then transferring a photoexcited electron to the semiconductor conduction band. The concomitant charge hole which is created on the dye is transferred to a liquid electrolyte or to a solid substrate functioning as hole conductor[7, 8]. Ruthenium(II) complexes are widely employed as dye sensitizers[9-11], delivering record efficiencies in DSCs devices[12-14]. The $\text{Ru}(\text{NCS})_2(\text{dcbpyH}_2)_2$ ($\text{dcbpyH}_2 = 4,4'$ -dicarboxyl- 2,2'-bipyridine) dye and its doubly deprotonated tetrabutylammonium salt, N3 and N719, respectively, have maintained a clear lead in DSCs technology, with efficiencies exceeding 11% [13, 15].

In these complexes, the thiocyanate ligands ensure fast regeneration of the photo-oxidized dye by the redox mediator, while the two equivalent 2,2'-bipyridine (bpy) ligands functionalized in their 4,4' positions by carboxylic groups ensure stable anchoring to the TiO_2 surface, allowing at the same time for the strong electronic coupling required for efficient excited state charge injection[13, 16, 17]. For further progress, however, higher conversion efficiencies need to be achieved. To this end, sensitizers and a deeper understanding of the interaction between the dye and the TiO_2 nanoparticle are essential.

A problem with the otherwise highly optimized homoleptic N3/N719 dyes is that their absorption is mainly centered in the blue and green spectral regions, substantially missing harvesting of photons in the red or near infrared region of the spectrum. Heteroleptic sensitizers have been therefore devised in which one of the two bpy's is specifically functionalized to obtain increased DSCs' performances, in particular their light harvesting capability[18-24]. Quite unexpectedly, however, experiments have shown that the photovoltaic performances of DSCs employing such

heteroleptic dyes are significantly lower compared to those observed using the parent homoleptic dyes[13, 18-20].

For this family of dyes, it was found that the photocurrent obtained from TiO_2 – sensitized films decreased when the fully protonated to fully deprotonated dyes were used to sensitize the semiconductor film[25]. The DSCs open circuit voltage, on the other hand, showed an opposite trend, increasing from the fully protonated to the fully deprotonated dye. An optimal product of photocurrent and open circuit voltage was found for an intermediate number of protons, which allowed further device optimization leading to efficiency exceeding 11% [13].

Recently, we have correlated the dye adsorption mode on TiO_2 with its photovoltaic performances; in particular, we found that heteroleptic dyes provide constantly reduced open circuit potentials compared to the homoleptic complex N719[26].

Experiments showed that the open-circuit potential of DSCs employing such heteroleptic dyes is significantly lower compared to that observed using the parent N719 dye, lying usually below 750 mV[11, 18, 20, 23, 27, 28]. In particular, a series of homogeneous DSCs fabricated under the same conditions and with the same TiO_2 paste/electrolyte formulation, but employing N719 or heteroleptic dyes[26], showed a consistently reduced open-circuit potential for cells employing the latter dyes, pointing at a precise dye effect in determining the cell open-circuit potential.

We found that heteroleptic dyes necessarily adsorb on TiO_2 using carboxylic groups residing on the same bpy ligand, while N719 effectively exploits three carboxylic groups residing on two different bipyridine ligands for grafting onto TiO_2 . We speculated that heteroleptic dyes, by means of their adsorption mode, induce an unfavorable interaction with the TiO_2 semiconductor which leads to a TiO_2 conduction band (CB) energy down-shift compared to homoleptic dyes, ultimately causing reduced photovoltages. This is possibly due to the unfavorable dipolar fields exerted on the TiO_2 surface[26, 29, 30], This analysis was somehow confirmed by a very recent study by some of us[31], where YE05 dye showing two equivalent bipyridine ligands (but replacing the thiocyanate ligands by a phenyl-pyridine cyclometallated ligand)[31] effectively delivered in DSCs an open

circuit potential of ca. 800 mV, close to the values of ca. 850 mV characteristic of highly optimized N719-based DSCs. As a matter of fact, heteroleptic dyes show open circuit potentials below 800 mV even in the most favorable cases.

Other than the TiO₂ CB shift due to the sensitizer electrostatic interaction, i.e. dipolar field, with the semiconductor, a further possible reason for the larger open circuit potential in homoleptic dyes is that they negatively charge the TiO₂ semiconductor by virtue of increased charge transfer from the three carboxylic groups contacting the surface, thus shifting the CB at higher energies[32]. Compared to heteroleptic complexes, homoleptic dyes can also form a more compact sensitizer monolayer on the TiO₂ surface again by virtue of their adsorption geometry, which might contribute to prevent electron recombination from TiO₂ to the oxidized electrolyte[33-35].

Altogether, these observations clearly suggest that the three carboxylic groups anchoring to TiO₂, as peculiar for N3/N719 and the YE-05 cyclometallated complex, are essential for high open circuit potentials. It is therefore highly desirable to design dyes which preserve the three anchoring groups, as so far possible only for homoleptic complexes, still allowing for shifting the dye absorption spectrum towards the red and/or increasing its molar absorption coefficient, as reported for heteroleptic complexes based on functionalized ancillary bipyridine ligands. To fulfill the above requirements we designed and synthesized mixed bipyridine ligands which bear one carboxylic group and one conjugated π -excessive heteroaromatic substituent at the 4 and 4' positions (Scheme 1). By employing these ligands we synthesized the corresponding heteroleptic complex in combination with 2,2'-bipyridine-4,4'-dicarboxylate and two thiocyanate ligands (Scheme 2). This complex carries three carboxylic groups and one functionalized 4-bpy position for tuning of the sensitizer electronic and optical properties.

In this paper, we report a combined experimental and theoretical study of a Ru(II) complex based on the mixed bipyridine ligand. We propose the synthesis of a dye, of formula Ru-LL1 (NCS)₂, where L=(4-4'-dicarboxy-2,2'-bipyridine) and L1= 4-carboxylate-4'-[(E)-2-EDOTvinyl]-2,2'-bpy, labeled **MB**, Scheme 2. In the synthesis of this dye based on mixed bipyridine ligands we wish to

exploit the “three anchoring sites” concept which seems to be responsible of the unmatched performances of the N719 dye. Indeed a dcbpy is substituted by 4-carboxylate-4'-[(*E*)-2-EDOTvinyl]-2,2'-bpy and then we introduce an additional carboxylic group.

2. Experimental details

2.1 General. NMR spectra were recorded on a Bruker AMX-500 instrument operating at 500.13 (¹H) and 125.77 MHz (¹³C). Coupling constants are given in Hz. ¹³C multiplicities were assigned on the basis of J-MOD experiments. High resolution mass spectra were recorded on a Bruker Daltonics ICR-FTMS APEX II spectrometer equipped with an electrospray ionization source. Flash chromatography was performed with Merck grade 9385 silica gel 230–400 mesh (60 Å). Reactions were performed under nitrogen in oven dried glassware and monitored by thin layer chromatography using UV light (254 nm and 365 nm) as visualizing agent. All reagents were obtained from commercial suppliers at the highest purity grade and used without further purification. Anhydrous solvent were purchased from Sigma Aldrich and used without further purification except for toluene that was degassed prior to use according to the freeze-pump-thaw procedure. Extracts were dried over Na₂SO₄ and filtered before removal of the solvent by evaporation.

2.2 Synthesis of ligand 2b.

Methyl 2-(trimethylstannyl) isonicotinate (5). Hexamethyldistannane (210 μL, 334 mg, 1.02 mmol) and tetrakis(triphenylphosphine)palladium (0) (70 mg, 0.06 mmol) were added to a solution of methyl 2-chloroisonicotinate (100 mg, 0.58 mmol) in toluene (10 ml) and the resulting mixture was refluxed for 3 h. AcOEt (50 mL) and water (100 mL) were added. The layers were separated, the organic layer was washed with water (5 x 100 mL), dried, and the solvent was removed by

rotary evaporation to leave an oily residue that was used for the next reaction without further purification.

Methyl 4-[2-(3,4-ethylenedioxythien-2-yl)vinyl]-2,2'-bipyridine-4'-carboxylate (2b). Stannilate⁵ (95 mg, 0.41 mmol) and bromo derivative **4**¹ (105 mg, 0.32 mmol) were dissolved in toluene (10 mL). Tetrakis(triphenylphosphine)palladium(0) (34 mg, 0.03 mmol) was added and the resulting mixture was refluxed for 20 h. A brown precipitate was collected upon filtration, extensively washed with toluene, and dried under vacuum, resulting in 85% pure **2b** (65 mg, 53%) which was used without further purification for the next reaction. ¹H NMR (CDCl₃) δ 8.97 (s, 1H), 8.87 (d, *J* = 4.9 Hz, 1H), 8.65 (d, *J* = 5.1 Hz, 1H), 8.48 (s, 1H), 7.91 (d, *J* = 4.2 Hz, 1H), 7.49 (d, *J* = 16.1 Hz, 1H), 7.37 (d, *J* = 4.4 Hz, 1H), 6.92 (d, *J* = 16.1 Hz, 1H), 6.36 (s, 1H), 4.36-4.34 (m, 2H), 4.28-4.26 (m, 2H), 4.01 (s, 3H). ¹³C NMR (CDCl₃) δ 165.8 (C, 1C), 157.3 (C, 1C), 156.8 (C, 1C), 149.9 (CH, 1C), 149.7 (CH, 1C), 146.1 (C, 1C), 142.1 (C, 2C), 138.5 (C, 1C), 123.3 (CH, 1C), 123.0 (CH, 1C), 122.9 (CH, 1C), 120.9 (CH, 1C), 120.6 (CH, 1C), 117.9 (CH 1C), 116.1 (C, 1C), 99.9 (CH, 1C), 64.9 (CH₂, 1C), 64.6 (CH₂, 1C), 52.7 (CH₃, 1C).

3. Results and discussion

3.1 Design and synthesis of the mixed ancillary ligand.

A number of donor-functionalized bpy ancillary ligands (type A, Scheme 3) have been so far reported in the literature, mostly carrying thiophene-based π -spacers[24]. In particular, we have described a number of ancillary bpy ligand conjugated with electron-rich and electron-poor heteroaromatic substituents[36]. Among these, a heteroleptic ruthenium complex containing an ancillary ligand carrying the electron-rich 3,4-ethylenedioxythiophene (EDOT) ring was used in DSCs, yielding a photovoltaic efficiency of 9.1%[23]. More recently, we have presented the example of a heteroarylvinylene π -conjugated quaterpyridine Ru(II) sensitizer (N1044), which

contained a conjugated EDOT moiety. The sensitizer, used in DSCs, exhibited an effective panchromatic absorption band, covering the entire visible spectrum up to the NIR region, and record IPCE curve ranging from 360 to 920 nm[37]. Based on these premises we have therefore designed the mixed ligand 4-carboxylate-4'-[(*E*)-2-EDOTvinyl]-2,2'-bpy **2a** and synthesized the corresponding heteroleptic complex [*cis*-(dithiocyanato)-Ru-(4,4'-dicarboxylate-2,2'-bpy)-[4-carboxylate-4'-[(*E*)-2-EDOTvinyl]-2,2'-bpy] **3**.

The precursor ligand **2b**, where the carboxylic functionality is protected via its methyl ester, was synthesized according to Scheme 4 via a Stille cross-coupling reaction of 4-[2-EDOTvinyl]-2-bromopyridine (**4**)[37] with methyl 2-(trimethylstannyl)isonicotinate (**5**), obtained through a Pd catalyzed stannylation with hexamethyldistannane[38] of commercially available methyl 2-chloroisonicotinate (**6**). The asymmetric ligand **2b** was isolated as a crude precipitate from the reaction mixture. Due to its poor solubility, purification via recrystallization or chromatography was not viable and the crude compound was used as such in the subsequent formation of the Ru(II) complex.

The heteroleptic complex **3** was prepared according to the route described in Scheme 5. The ruthenium complex was obtained as a mixture of two isomers, whose structures are depicted in Scheme 6, which we have not been able to separate despite various attempts with a Sephadex column.

3.2 Electronic structure and optical properties

To gain insight into the electronic and optical properties of the investigated sensitizer, we performed Density Functional Theory/ Time Dependent Density Functional Theory (DFT/TDDFT) calculations in vacuum and ethanol solution. All the calculations have been performed by the GAUSSIAN 09 (G09) program package[39]. We optimized the molecular structure of MB in vacuum using the B3LYP exchange–correlation functional[40] and a 3-21G* basis set[41]. TDDFT calculations of the lowest singlet–singlet excitations were performed in ethanol solution on the

structure optimized in vacuum and using a DGDZVP basis set[42]. The nonequilibrium version of C-PCM[43-45] was employed for TDDFT calculations, as implemented in G09. To simulate the optical spectra, the 50 lowest spin-allowed singlet–singlet transitions were computed on the ground state geometry. Transition energies and oscillator strengths were interpolated by a Gaussian convolution with an σ value of 0.20 eV.

Since the synthesis we obtained a mix of two isomers, we simulated the electronic and optical properties of both compounds. To avoid possible misinterpretations of the data due to the different dye protonation, we considered only the totally deprotonated species. To assess the stability of different isomers we compared their energy in solution, as obtained from DFT calculations. As expected from the synthesis results, the two isomers present approximately the same stability, the MB_1 is only 0.04 kcal/mol more stable compared to MB_2. We then investigated the electronic structure of both isomers; a schematic representation of the energy levels and the isodensity plots of selected frontier molecular orbitals of MB_1 complexes are shown in Figure 1. For comparison we also investigated the N3 complex considering the totally deprotonated species.

The set of quasidegenerate Highest Occupied Molecular Orbitals (HOMO, HOMO-1 and HOMO-2) of all the investigated complexes have essentially Ru t_{2g} character while the Lowest Unoccupied Molecular Orbitals (LUMOs) of the complexes are bipyridine π^* orbitals. For the three considered complexes, we note that the HOMO level are essentially the same energy (5.08-5.02 eV) because are the same orbitals, while the LUMO level of N3 are destabilized by 0.37 eV respect to the LUMO of MB. This destabilization is due to the different localization of the LUMO orbitals, which in MB are localized on the L1 ligand, while in the N3 the LUMOs are delocalized on both bipyridine ligands[16].

The UV-vis absorption spectrum of the MB complex is compared to that of the standard deprotonated dye [15, 46] in Figure 2. As it can be noticed, the MB dye shows an absorption maximum at 534 nm, 0.11 eV red shifted absorption compared to N3 ($\lambda_{\max} = 510$ nm) and also

shows a substantially more intense band on the blue-wing of the spectrum. This confirms that the introduction of the mixed bipyridine ligand in the MB complex effectively achieves the desired enhancement of the dye light-harvesting capability.

We now move to the calculated optical properties of the investigated systems. The absorption spectra for the investigated MB₁ and MB₂ species have been computed throughout the visible and UV region, thus allowing us to compare calculated and experimental data, the results are reported in Figure 3.

As it can be noticed, the two MB isomers have rather different optical properties in the long wavelength region (500-600 nm). For both compounds, MB₁ and MB₂, in this region we computed the same transitions (at 615nm) even if with different oscillator strength (f), 0.0113 and 0.1288, respectively. On the other hand both isomers present a similar absorption for the bands computed at ca. 530 and 410 nm. Comparing Figure 2 and 3, we notice the best match with the experimental spectrum is obtained for the 1:1 average spectrum of the two isomers, although the calculated spectrum of MB₁ also resembles the experimental one while that of MB₂ shows rather different features.

To better visualize this and to assign the experimental spectrum, we report in Figure 4 a comparison between the experimental and calculated spectra for MB₁. For the MB₁ species, the first band, experimentally found at 534 nm, is computed at 528 nm, only 0.03 eV blue-shifted with respect to the experimental data, and appears to be composed of two transitions at 551 and 530 nm, which originated from the HOMO-1/HOMO (Ru-SCN) couple to the LUMO (π^* on L1). We assign the transitions as having Metal to Ligand Charge Transfer (MLCT) character. The second band, experimentally found at 389 nm, is computed at 411 nm only 0.17 eV red-shifted with respect to the experimental data, and is composed essentially by one transitions at 413 nm, which originated from the HOMO-3/HOMO (NCS-EDOT/Ru-SCN) couple to the LUMO/LUMO+2 (π^* on L1). We assign this transitions as having mixing $\pi \rightarrow \pi^*/MLCT$ character. The third band, experimentally

found at 313 nm, is computed at 343 nm 0.34 eV red-shifted with respect to the experimental data, and is composed essentially by one transitions at 339 nm, which originated from the HOMO-3 (NCS-EDOT) couple to the LUMO+2 (π^* on L1). We assign this transitions as having $\pi \rightarrow \pi^*$ character.

3.3 Dye adsorption on TiO₂ and electronic structure

To check whether the proposed dye design could effectively lead to dye adsorption on TiO₂ by means of three anchoring groups, we calculated the interaction between the MB_1 dye and a model (TiO₂)₃₈ nanoparticle[48, 49]. Geometry optimizations of the dye@TiO₂ complex were performed by the ADF code[50] using the PBE exchange-correlation potential and a DZ basis set for all atoms. To check the influence of dye protonation on the interaction with the TiO₂ surface we modeled the dyes carrying 1, 2 and 3 protons, the latter corresponding to the neutral complex. The resulting optimized geometries are reported in Figure 5.

As it can be noticed, out of the three carboxylic groups, the dye maintains in all cases one bridged bidentate adsorption and two monodentate adsorption modes, which can be protonated (as in the case with 3 protons) and/or hydrogen-bonding to surface-bound protons (e.g. for the case with 2 and 3 protons). This type of interaction with the TiO₂ surface is similar to what was found for the N719 dye on the same (TiO₂)₃₈ model and on a larger (TiO₂)₈₂ model[17], suggesting an effectively similar type of interfacial properties.

We then evaluated the electronic properties of the dye-sensitized TiO₂ models by performing B3LYP/DGDZVP single point calculations in ethanol solution on the optimized structures of the MB_1 dye adsorbed on TiO₂, considering 1, 2 and 3 protons. For comparative purposes, we also performed a similar calculation for the N3 dye on the same TiO₂ model carrying 3 protons. The results are reported in Figure 6. As it can be noticed, by increasing the number of protons carried by the dye, an energy down-shift of the TiO₂ conduction band (CB) is observed. Notice that this effect

is not limited to the CB edge but it involves the entire manifold of unoccupied states. This proton-induced TiO_2 CB down-shift has already been documented [17] and is related to the Nernstian dependence of the TiO_2 flat band potential upon the pH, with a reported CB energy down-shift by reducing the pH.

It is also interesting to compare our calculated data for MB_1 against the same data obtained for the prototypical N3 dye. For the sake of comparison we focus here on the system carrying 3 protons. The results, reported in Figure 6, show essentially the same TiO_2 CB DOS for the MB_1 and the N3 dye (the two DOS curves are almost superimposable), indicating that the details of the dye structure only slightly modulate the TiO_2 CB DOS by virtue of the dye dipole. The TiO_2 CB DOS is on the other hand sizably affected by the dye adsorption mode and by the dye coverage[32], in addition to the number of surface-adsorbed protons, as discussed above.

4. Conclusions

We have reported the design, synthesis and computational investigation of a class of Ru(II)- dyes based on mixed bipyridine ligands for use in dye-sensitized solar cells. These dyes were designed to preserve the optimal anchoring mode of the prototypical N719 sensitizer by three carboxylic groups, yet allowing for tunable optimization of their electronic and optical properties by selective substitution at one of the 4-4' positions of a single bipyridine ligand with π -excessive heteroaromatic groups. A problem with the otherwise highly optimized homoleptic N3/N719 dyes is indeed that their absorption is mainly centered in the blue and green spectral regions, substantially missing harvesting of photons in the red or near infrared region of the spectrum. Heteroleptic sensitizers have been therefore devised in which one of the two bitys is specifically functionalized to obtain increased DSCs' performances, in particular their light harvesting capability. Quite unexpectedly, however, experiments have shown that the photovoltaic performances, especially the open circuit voltage, of DSCs employing such heteroleptic dyes are

significantly lower compared to those observed using the parent homoleptic dyes. Thus the design rule we propose here combines the three anchoring site of N719 and the enhanced light-harvesting and flexibility of heteroleptic dyes. We thus synthesized a mixed bipyridine L1 ligand (4-carboxylate-4'-[(*E*)-2-EDOTvinyl]-2,2'-bpy) and the corresponding Ru-LL1 (NCS)₂ complex, labeled MB, where L=(4-4'-dicarboxy-2,2'-bipyridine). Unfortunately, the synthesis of the ruthenium complex led to a mixture of isomers (MB_1 and MB_2) which have not been possible to separate, thus preventing a precise characterization of this dye. We then resorted to DFT/TDDFT calculations to analyze the electronic structure and optical properties of this dye and to investigate the dye adsorption mode on a TiO₂ nanoparticle model. The best match between calculated data and the experimental absorption spectrum of the crude complex was found with the 1:1 average of the calculated spectra for the two isomers, in line with the results of the synthesis.

Our computational analysis shows that we are effectively able to introduce three carboxylic anchoring units into the dye, which are exploited for dye anchoring, and achieve at the same time an enhanced dye light harvesting, demonstrating the design concept. Upon solving the synthetic challenges associated with the obtainment of the pure complex we expect this class of dyes to deliver enhanced photovoltaic performances compared to standard ruthenium dyes.

Acknowledgements

We thank FP7-ENERGY 2010, Project 261910 “ESCORT” for financial support.

References:

- [1] M. Grätzel, Nature 414 (2001) 338.
- [2] A. Hagfeldt, M. Grätzel, Chem. Rev. 95/1 (1995) 49.
- [3] P.V. Kamat, J. Phys. Chem. C 111/7 (2007) 2834.

- [4] M.K. Nazeeruddin, Q. Wang, L. Cevey, V. Aranyos, P. Liska, E. Figgemeier, C. Klein, N. Hirata, S. Koops, S.A. Haque, J.R. Durrant, A. Hagfeldt, A.B.P. Lever, M. Grätzel, *Inorg. Chem.* 45/2 (2005) 787.
- [5] B. O'Regan, M. Grätzel, *Nature* 353/6346 (1991) 737.
- [6] J.M. Rehm, G.L. McLendon, Y. Nagasawa, K. Yoshihara, J. Moser, M. Grätzel, *J. Phys. Chem.* 100/23 (1996) 9577.
- [7] M. Grätzel, *Inorg. Chem.* 44/20 (2005) 6841.
- [8] A. Hagfeldt, G. Boschloo, L. Sun, L. Kloo, H. Pettersson, *Chem. Rev.* 110/11 (2010) 6595.
- [9] M. Grätzel, *C. R. Chimie* 9/5-6 (2006) 578.
- [10] M. Grätzel, *Acc. Chem. Res.* 42/11 (2009) 1788.
- [11] J.-F. Yin, M. Velayudham, D. Bhattacharya, H.-C. Lin, K.-L. Lu, *Coord. Chem. Rev.* 256/23-24 (2012) 3008.
- [12] L. Han, A. Islam, H. Chen, C. Malapaka, B. Chiranjeevi, S. Zhang, X. Yang, M. Yanagida, *Energy Environ. Sci.* 5/3 (2012) 6057.
- [13] F. De Angelis, S. Fantacci, A. Selloni, M.K. Nazeeruddin, *Chem. Phys. Lett.* 415/1-3 (2005) 115.
- [14] Y. Cao, Y. Bai, Q. Yu, Y. Cheng, S. Liu, D. Shi, F. Gao, P. Wang, *J. Phys. Chem. C* 113/15 (2009) 6290.
- [15] M.K. Nazeeruddin, A. Kay, I. Rodicio, R. Humphry-Baker, E. Mueller, P. Liska, N. Vlachopoulos, M. Grätzel, *J. Am. Chem. Soc.* 115/14 (1993) 6382.
- [16] S. Fantacci, F. De Angelis, A. Selloni, *J. Am. Chem. Soc.* 125/14 (2003) 4381.
- [17] F. De Angelis, S. Fantacci, A. Selloni, M.K. Nazeeruddin, M. Grätzel, *J. Phys. Chem. C* 114/13 (2010) 6054.
- [18] M.K. Nazeeruddin, S.M. Zakeeruddin, J.J. Lagref, P. Liska, P. Comte, C. Barolo, G. Viscardi, K. Schenk, M. Grätzel, *Coord. Chem. Rev.* 248/13-14 (2004) 1317.

- [19] J.N. Clifford, E. Palomares, M.K. Nazeeruddin, M. Grätzel, J.R. Durrant, *J. Phys. Chem. C* 111/17 (2007) 6561.
- [20] P. Wang, C.d. Klein, R. Humphry-Baker, S.M. Zakeeruddin, M. Grätzel, *J. Am. Chem. Soc.* 127/3 (2005) 808.
- [21] F. Gao, Y. Wang, D. Shi, J. Zhang, M. Wang, X. Jing, R. Humphry-Baker, P. Wang, S.M. Zakeeruddin, M. Grätzel, *J. Am. Chem. Soc.* 130/32 (2008) 10720.
- [22] C.-Y. Chen, S.-J. Wu, C.-G. Wu, J.-G. Chen, K.-C. Ho, *Angew. Chem. Int. Ed.* 45/35 (2006) 5822.
- [23] A. Abbotto, C. Barolo, L. Bellotto, F. De Angelis, M. Grätzel, N. Manfredi, C. Marinzi, S. Fantacci, J.-H. Yum, M.K. Nazeeruddin, *Chem. Comm.* 0/42 (2008) 5318.
- [24] A. Abbotto, N. Manfredi, *Dalton Trans.* 40/46 (2011) 12421.
- [25] M.K. Nazeeruddin, M. Grätzel, *Molecular and Supramolecular Photochemistry*, Marcel Dekker, New York, 2003.
- [26] F. De Angelis, S. Fantacci, A. Selloni, M. Grätzel, M.K. Nazeeruddin, *Nano Lett.* 7/10 (2007) 3189.
- [27] C.Y. Chen, S.J. Wu, J.Y. Li, C.G. Wu, J.G. Chen, K.C. Ho, *Adv. Mater.* 19/22 (2007) 3888.
- [28] M.K. Nazeeruddin, T. Bessho, L. Cevey, S. Ito, C. Klein, F. De Angelis, S. Fantacci, P. Comte, P. Liska, H. Imai, M. Graetzel, *J. Photochem. Photo. A* 185/2-3 (2007) 331.
- [29] P. Chen, J.H. Yum, F.D. Angelis, E. Mosconi, S. Fantacci, S.-J. Moon, R.H. Baker, J. Ko, M.K. Nazeeruddin, M. Grätzel, *Nano Lett.* 9/6 (2009) 2487.
- [30] S. Rühle, M. Greenshtein, S.G. Chen, A. Merson, H. Pizem, C.S. Sukenik, D. Cahen, A. Zaban, *J. Phys. Chem. B* 109/40 (2005) 18907.
- [31] T. Bessho, E. Yoneda, J.-H. Yum, M. Guglielmi, I. Tavernelli, H. Imai, U. Rothlisberger, M.K. Nazeeruddin, M. Grätzel, *J. Am. Chem. Soc.* 131/16 (2009) 5930.
- [32] E. Ronca, M. Pastore, L. Belpassi, F. Tarantelli, F. De Angelis, *Energy Environ. Sci.* 6/1 (2013) 183.

- [33] M. Miyashita, K. Sunahara, T. Nishikawa, Y. Uemura, N. Koumura, K. Hara, A. Mori, T. Abe, E. Suzuki, S. Mori, *J. Am. Chem. Soc.* 130/52 (2008) 17874.
- [34] M. Planells, L. Pelleja, J.N. Clifford, M. Pastore, F. De Angelis, N. Lopez, S.R. Marder, E. Palomares, *Energy Environ. Sci.* 4/5 (2011) 1820.
- [35] M. Pastore, F.D. Angelis, *ACS Nano* 4/1 (2009) 556.
- [36] A. Abbotto, L. Bellotto, F. De Angelis, N. Manfredi, C. Marinzi, *Eur. J. Org. Chem.* 2008/30 (2008) 5047.
- [37] A. Abbotto, F. Sauvage, C. Barolo, F. De Angelis, S. Fantacci, M. Grätzel, N. Manfredi, C. Marinzi, M.K. Nazeeruddin, *Dalton Trans.* 40/1 (2011) 234.
- [38] M. Benaglia, S. Toyota, C.R. Woods, J.S. Siegel, *Tetrahedron Lett.* 38/27 (1997) 4737.
- [39] M.J.T. Frisch, G. W.; Schlegel, H. B.; Scuseria, G. E.; Robb, M. A.; Cheeseman, J. R.; Scalmani, G.; Barone, V.; Mennucci, B.; Petersson, G. A.; Nakatsuji, H.; Caricato, M.; Li, X.; Hratchian, H. P.; Izmaylov, A. F.; Bloino, J.; Zheng, G.; Sonnenberg, J. L.; Hada, M.; Ehara, M.; Toyota, K.; Fukuda, R.; Hasegawa, J.; Ishida, M.; Nakajima, T.; Honda, Y.; Kitao, O.; Nakai, H.; Vreven, T.; Montgomery, Jr., J. A.; Peralta, J. E.; Ogliaro, F.; Bearpark, M.; Heyd, J. J.; Brothers, E.; Kudin, K. N.; Staroverov, V. N.; Kobayashi, R.; Normand, J.; Raghavachari, K.; Rendell, A.; Burant, J. C.; Iyengar, S. S.; Tomasi, J.; Cossi, M.; Rega, N.; Millam, J. M.; Klene, M.; Knox, J. E.; Cross, J. B.; Bakken, V.; Adamo, C.; Jaramillo, J.; Gomperts, R.; Stratmann, R. E.; Yazyev, O.; Austin, A. J.; Cammi, R.; Pomelli, C.; Ochterski, J. W.; Martin, R. L.; Morokuma, K.; Zakrzewski, V. G.; Voth, G. A.; Salvador, P.; Dannenberg, J. J.; Dapprich, S.; Daniels, A. D.; Farkas, Ö.; Foresman, J. B.; Ortiz, J. V.; Cioslowski, J.; Fox, D. J. , Gaussian, Inc., Wallingford CT, 2009.
- [40] A.D. Becke, *J. Chem. Phys.* 98 (1993) 5648.
- [41] J.S. Binkley, J.A. Pople, W.J. Hehre, *J. Am. Chem. Soc.* 102/3 (1980) 939.
- [42] N. Godbout, D.R. Salahub, J. Andzelm, W. Erich, *Can. J. Chem.* 70/2 (1992) 560.
- [43] M. Cossi, V. Barone, *J. Chem. Phys.* 115/10 (2001) 4708.
- [44] M. Cossi, V. Barone, R. Cammi, J. Tomasi, *Chem. Phys. Lett.* 255/4-6 (1996) 327.

- [45] S. Miertš, E. Scrocco, J. Tomasi, Chem. Phys. 55/1 (1981) 117.
- [46] M.K. Nazeeruddin, S.M. Zakeeruddin, R. Humphry-Baker, M. Jirousek, P. Liska, N. Vlachopoulos, V. Shklover, C.-H. Fischer, M. Grätzel, Inorg. Chem. 38/26 (1999) 6298.
- [47] G. Pizzoli, M.G. Lobello, B. Carlotti, F. Elisei, M.K. Nazeeruddin, G. Vitillaro, F. De Angelis, Dalton Trans. 41/38 (2012) 11841.
- [48] P. Persson, R. Bergström, S. Lunell, J. Phys. Chem. B 104/44 (2000) 10348.
- [49] F. De Angelis, A. Tilocca, A. Selloni, J. Am. Chem. Soc. 126/46 (2004) 15024.
- [50] G. te Velde, F.M. Bickelhaupt, E.J. Baerends, C. Fonseca Guerra, S.J.A. van Gisbergen, J.G. Snijders, T. Ziegler, J. Comput. Chem. 22/9 (2001) 931.

List of scheme, figure and table captions:

Scheme 1: Ligand design paradigm for Ru(II)-sensitizers. Left: two differently functionalized bipyridine ligands for heteroleptic complexes. Right: ligand design for Ru(II)-sensitizers including homoleptic and heteroleptic dyes.

Scheme 2. Chemical structure of the **MB** ruthenium sensitizer. Notice the three carboxylic anchoring groups.

Scheme 3. Chemical structure of the 4,4'-bis[(E)-2-(3,4-ethylenedioxythien-2-yl)vinyl]-2,2'-bipyridine (**1**) and 4-carboxylate-4'-[(E)-2-EDOTvinyl]-2,2'-bpy (**2**).

Scheme 4. Synthesis of the methyl ester protected ancillary mixed ligand **2b**.

Scheme 5. Synthetic route used for the MB sensitizer.

Scheme 6. Chemical structure of isomers MB_1 and MB_2

Figure 1. Schematic representation of the energy levels of the MB_1, MB_2 and N3 complexes, considering energies in ethanol solution. Isodensity surface plots (isodensity contour: 0.035 a.u.) of selected MB_1 molecular orbitals are also shown.

Figure 2. Experimental absorption spectra of the deprotonated **MB** (black lines) and **N3**[47] (blue lines) dyes measured in ethanol solution.

Figure 3. Top: Calculated UV-vis absorption spectrum for MB_1. Middle: Calculated UV-vis absorption spectrum for MB_2. Vertical red lines correspond to calculated excitation energies and oscillator strengths. Bottom: Average absorption spectrum of MB_1 and MB_2 in 1:1 ratio.

Figure 4. Comparison between the simulated spectrum of **MB_1** (red line) and the experimental spectrum (black line). Vertical red lines correspond to calculated excitation energies and oscillator strengths.

Figure 5. Optimized geometrical structures for the MB_1 dye adsorbed onto a (TiO₂)₃₈ nanoparticle model. Top, middle and bottom panels refer to the dye carrying 1, 2 and 3 protons, respectively.

Figure 6. Upper panel: Calculated density of states (DOS) in the TiO₂ conduction band region for the MB_1 dye adsorbed onto a (TiO₂)₃₈ nanoparticle model, carrying 1, 2 and 3 protons. Bottom: Comparison between the DOS calculated for MB_1 and N3, both carrying 3 protons.

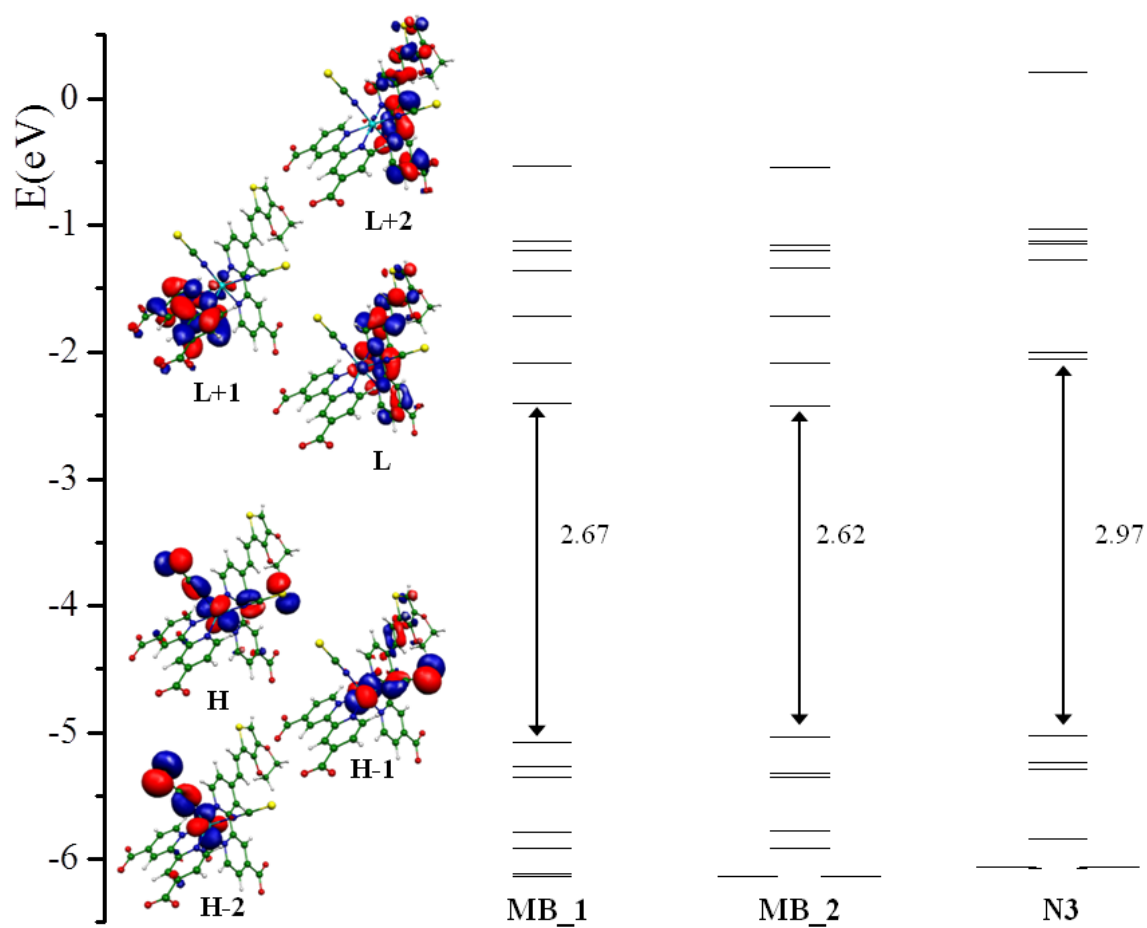


Figure 1

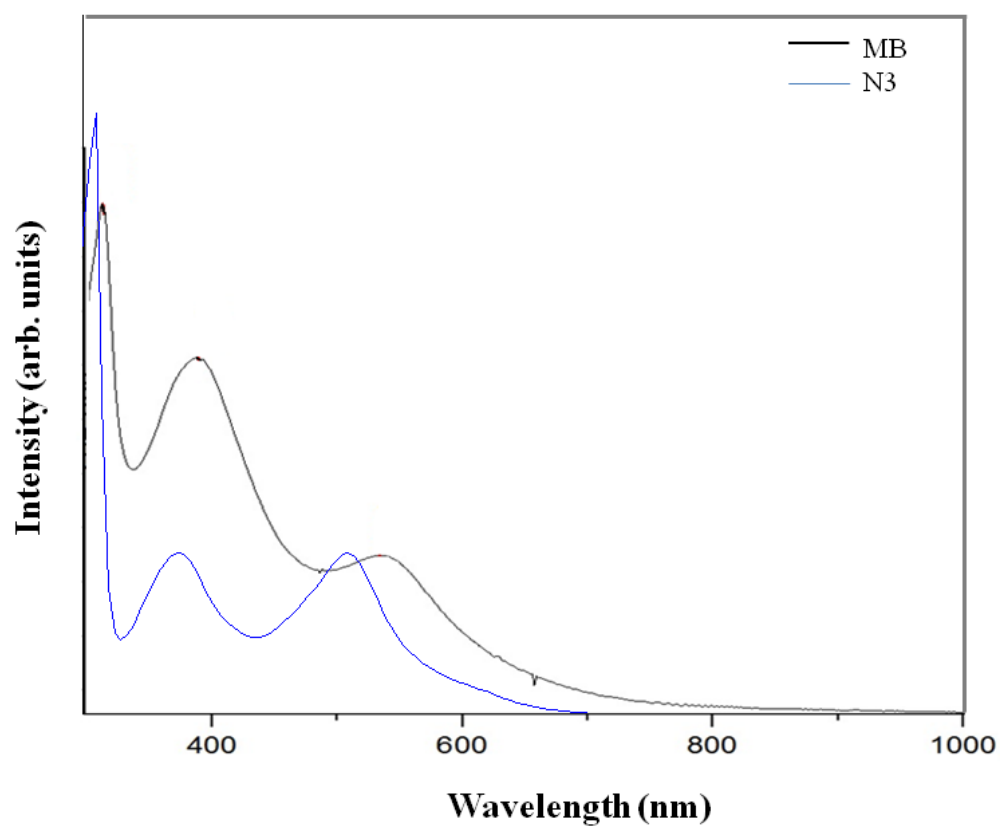


Figure 2

ACCEPTED

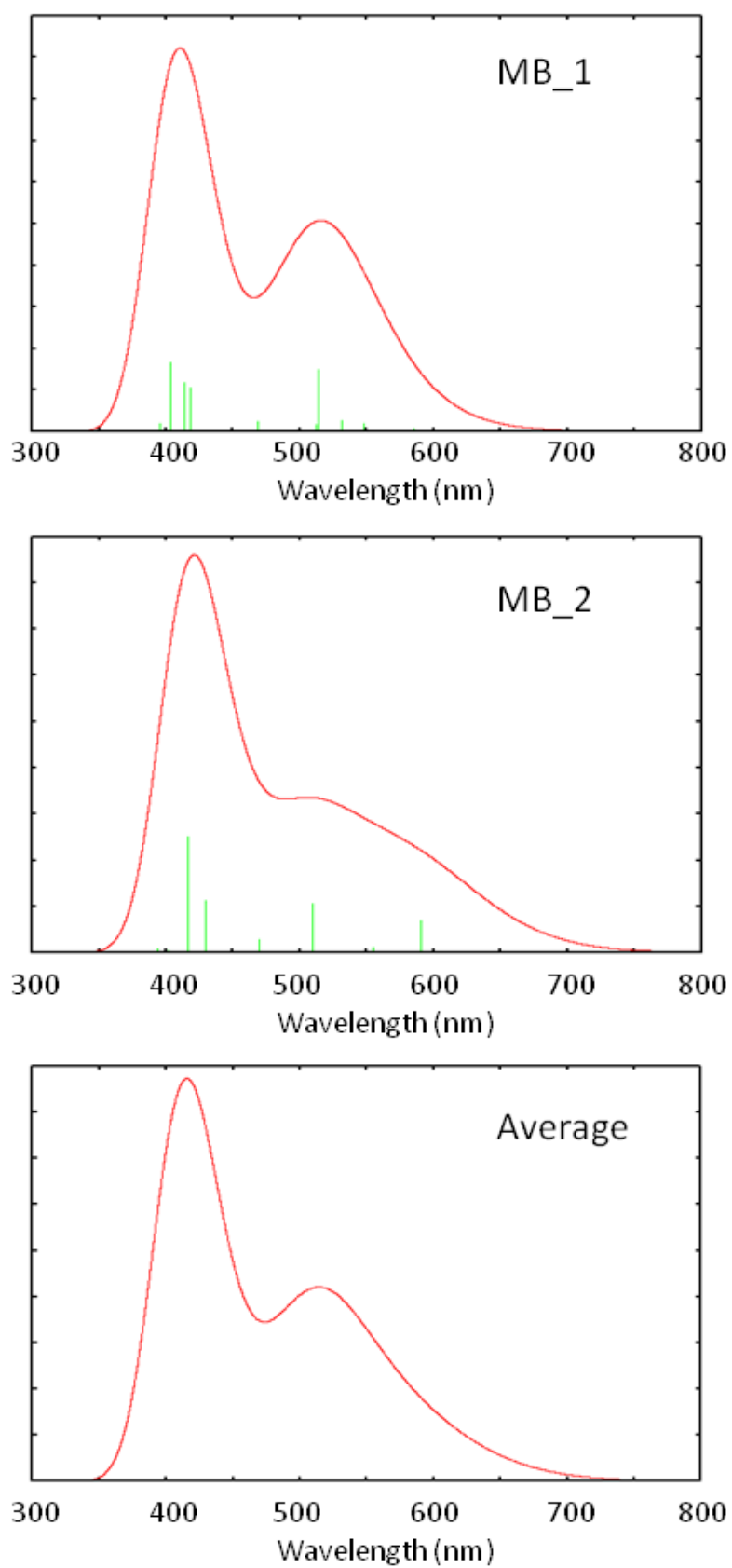


Figure 3

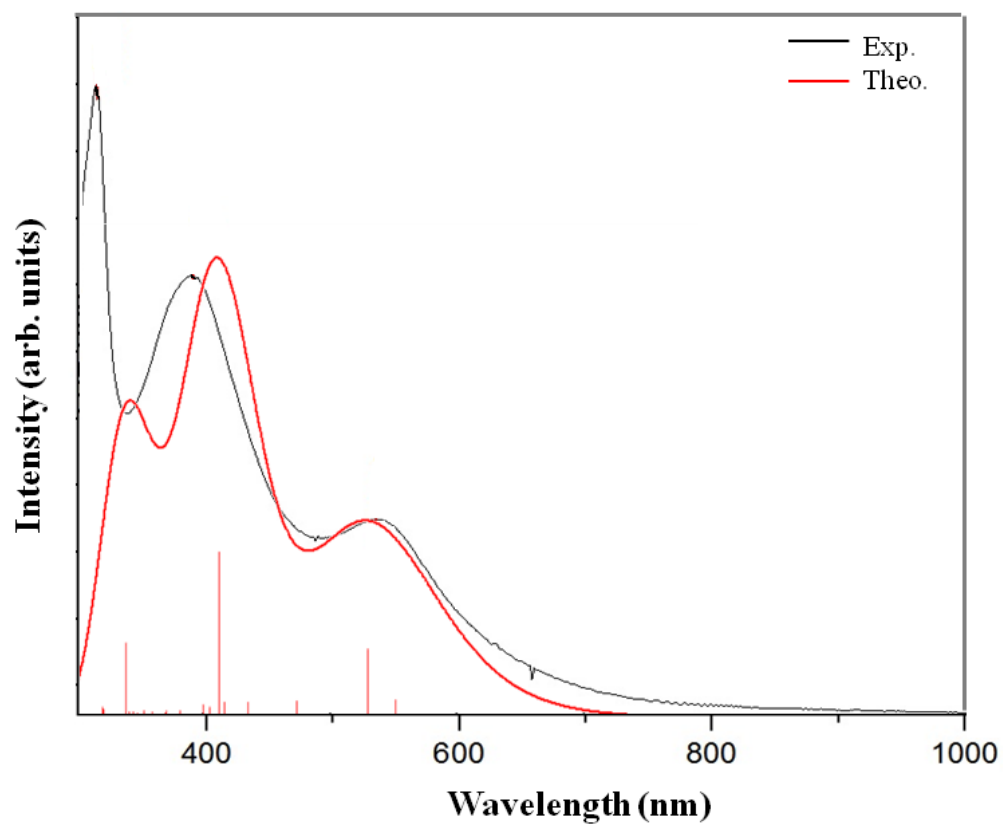


Figure 4

ACCEPTED

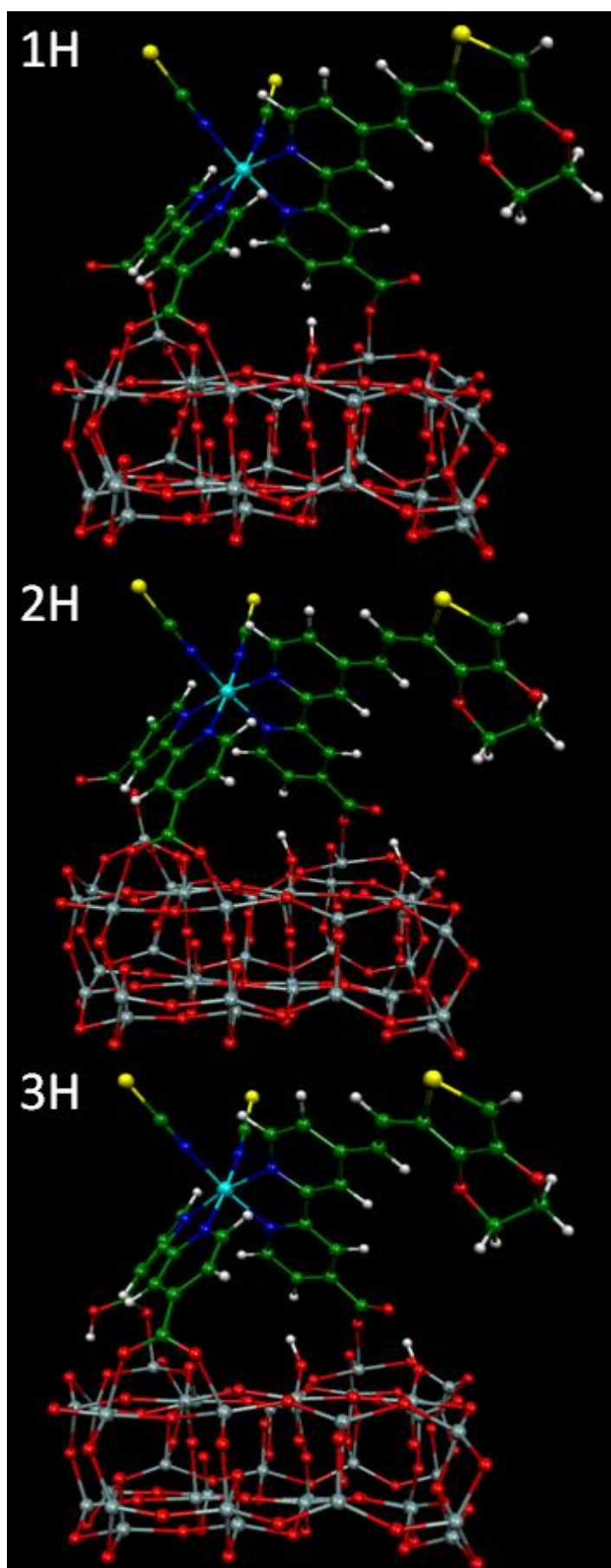


Figure 5

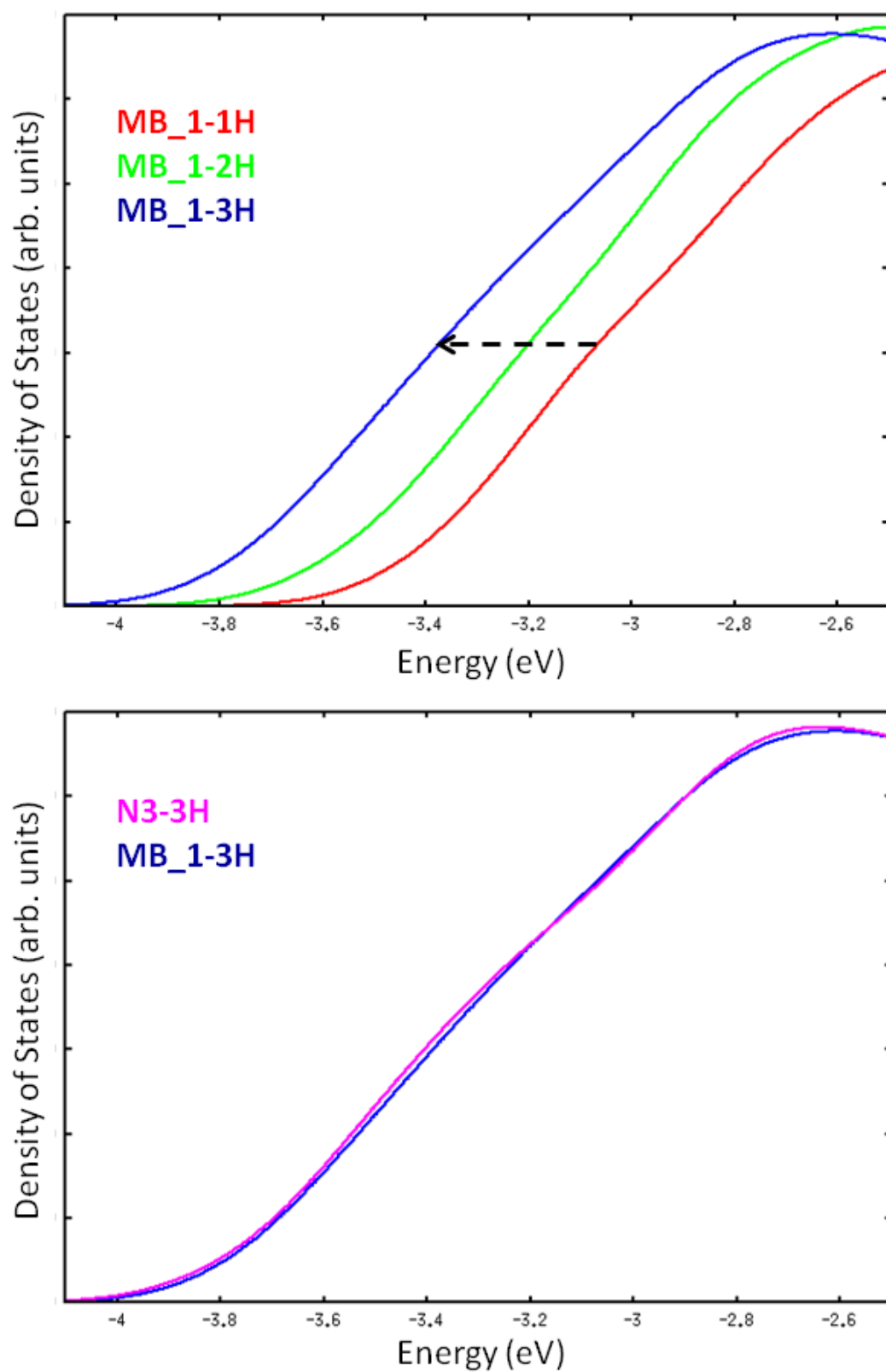
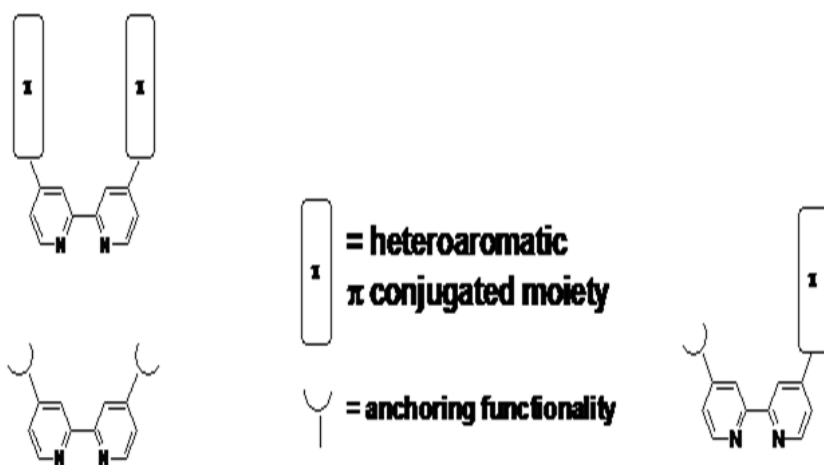
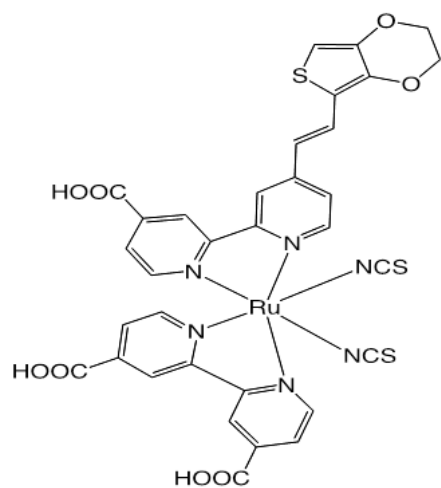


Figure 6



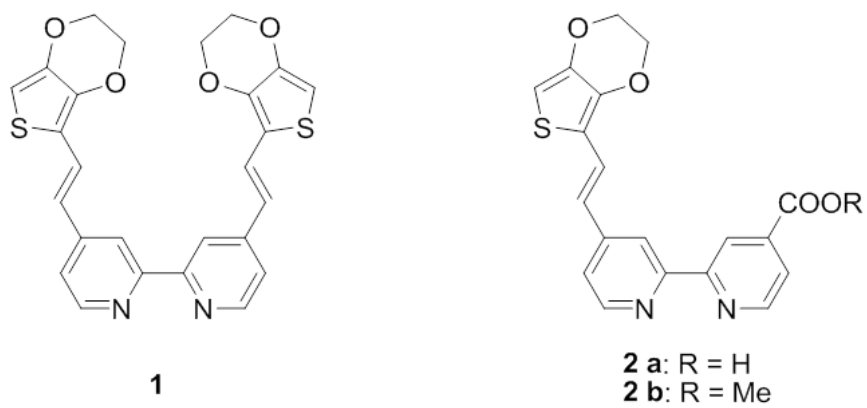
Scheme 1

ACCEPTED



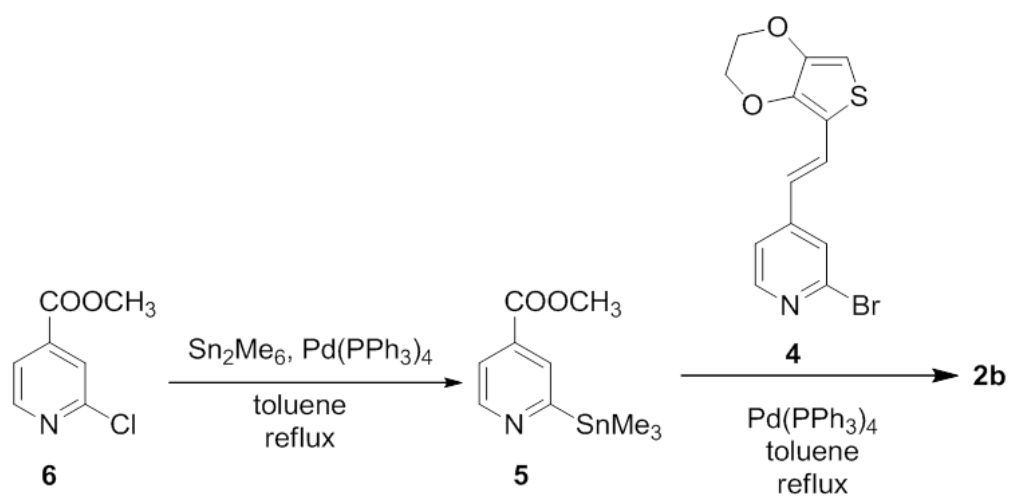
Scheme 2

ACCEPTED



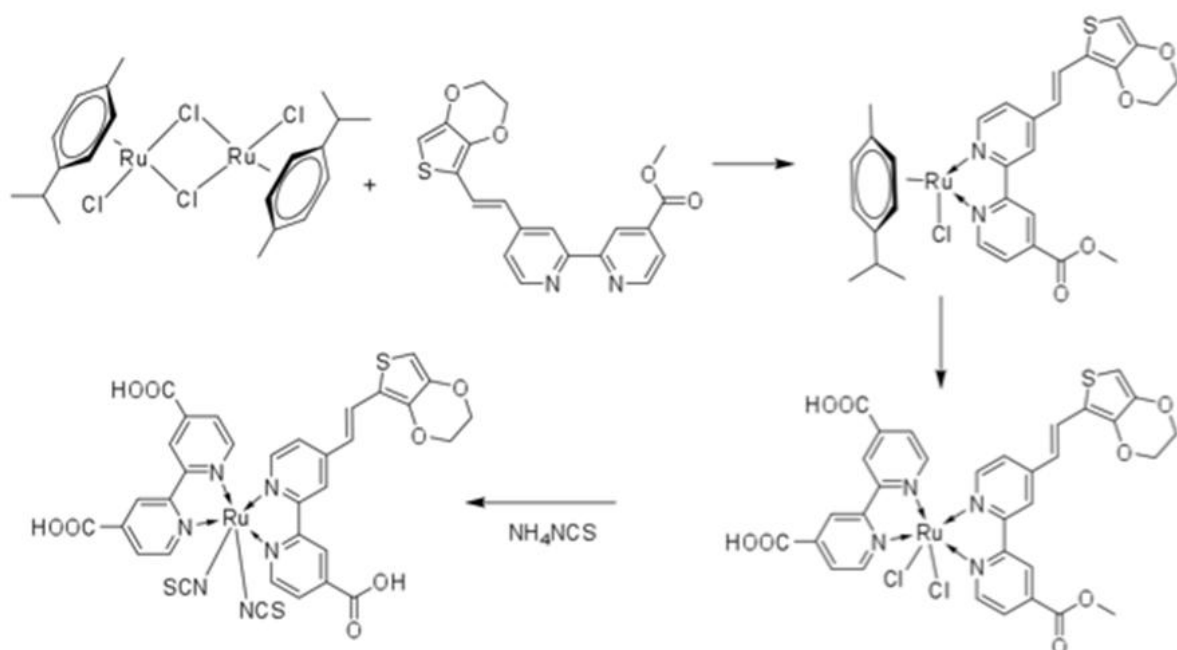
Scheme 3

ACCEPTED



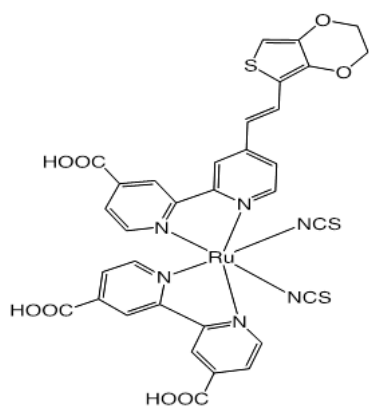
Scheme 4

ACCEPTED

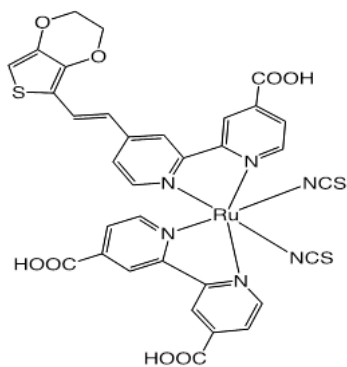


Scheme 5

ACCEPTED



MB_1



MB_2

Scheme 6

ACCEPTED

Highlights

We designed a heteroleptic Ru(II) sensitizers with three carboxylic anchoring groups.

The three carboxylic anchoring groups are essential for high open circuit potentials.

Introduction of the mixed bipyridine ligand increases the dye light absorption.

Computational simulations confirm the three anchoring sites on TiO₂.

ACCEPTED MANUSCRIPT